Title
Goos-Hänchen Shift and Even–Odd Peak Oscillations in Edge-Reflections of Surface Polaritons in Atomically Thin Crystals

Journal
Nano Letters, 17(3)

ISSN
1530-6984

Authors
Kang, Ji-Hun
Wang, Sheng
Shi, Zhiwen
et al.

Publication Date
2017-03-08

DOI
10.1021/acs.nanolett.6b05077

Peer reviewed

Goos-Hänchen shift and even-odd peak oscillations in edge-reflections of surface polaritons in atomically thin crystals

Ji-Hun Kang[1,2†], **Sheng Wang**[1,3†], **Zhiwen Shi**[4,5*], **Wenyu Zhao**[1,6], **Eli Yablonovitch**[3,7,8], **and Feng Wang**[1,3,8*]

[1] Department of Physics, University of California at Berkeley, Berkeley, California 94720, USA

[2] Department of Physics, Korea University, Seoul 136-701, Korea

[3] Materials Science Division, Lawrence Berkeley National Laboratory, Berkeley, California 94720, USA

[4] Key Laboratory of Artificial Structures and Quantum Control (Ministry of Education), Department of Physics and Astronomy, Shanghai Jiao Tong University, Shanghai 200240, China

[5] Collaborative Innovation Center of Advanced Microstructures, Nanjing 210093, China

[6] Department of Physics, Harbin Institute of Technology, Harbin 150001, China

[7] Department of Electrical Engineering and Computer Science, University of California at Berkeley, Berkeley, California 94720, USA

[8] Kavli Energy NanoSciences Institute at the University of California, Berkeley and the Lawrence Berkeley National Laboratory, Berkeley, California 94720, USA

[†]These authors contributed equally to this work

[*]fengwang76@berkeley.edu; zhiwen22@gmail.com

Two-dimensional surface polaritons (2DSPs), such as graphene plasmons, exhibit various unusual properties, including electrical tunability[1–5], strong spatial confinement with high Q-factor[6–9], which can enable tuneable photonic devices for deep sub-wavelength light manipulations[10]. Reflection of plasmons at the graphene's edge plays a critical role in the manipulation of 2DSP and enabled their direct visualization in near-field infrared microscopy[4,5]. However, a quantitative understanding of the edge-reflections, including reflection phases and diffraction effects, has remained elusive. Here, we show theoretically and experimentally that edge-reflection of 2DSP exhibits unusual behaviours due to the presence of the evanescent waves, including an anomalous Goos-Hänchen phase shift as in total internal reflections and an unexpected even-odd peak amplitude oscillation from the wave diffraction at the edge. Our theory is not only valid for plasmons in graphene, but also for other 2D polaritons, such as phonon polaritons in ultrathin boron nitride flakes[11,12] and exciton polariton in two-dimensional semiconductors[13–17].

Reflection is a fundamental phenomenon of electromagnetic (EM) waves. Surface reflection and interference of multiple reflected waves lie at the heart of Fabry-Perot resonances, and total internal reflection can exhibit an unusual Goos-Hänchen phase shift due to the existence of evanescent waves[18,19]. Reflection is not limited to the three-dimensional plane waves, but can also be observed in two-dimensional surface polaritons(2DSPs)[20]. Specifically, recent studies on near-field spectroscopy of 2DSPs bound to the atomically thin crystals such as graphene and boron nitride flakes exhibit strong reflection at edges[4,7,11,12]. Due to the sudden disappearance of surface conductivity at the edge, no propagation waves exist on the other side of the edge and it is often simply assumed that the reflection will have a simple 0 or π phase shift. However, detailed experiments don't match with this simple assumption, and a strange "even-odd" peak oscillation in the interference pattern is also observed (refs). To explain these anomalous phenomena, complex mechanisms like "modified plasmon wavelength" and "edge-excitation of plasmons" were invoked[7,21–23]. Here we show that these anomalous phenomena are intrinsic to edge reflection of 2DSPs due to the presence of near-field evanescent waves at the edge of 2D crystals. Goos-Hänchen phase shifts associated with the evanescent waves lead to an apparent plasmon wavelength modification, and the interference between the propagating and evanescent waves produces the even-odd peak oscillations. These results are essential for quantitative understanding of reflection of 2DSPs and for their applications in ultra-small polaritonic resonators[1,24–27].

Experimentally we investigated plasmon reflection in bare graphene on top of SiO_2/Si substrates and graphene sandwiched between hBN flakes. The bare graphene sample allows us to determine the edge position from topography image reliably for quantitative

evaluation of the phase shift, while the sandwiched graphene samples have much higher quality factor and allows for detailed examination of plasmon interference patterns. Plasmons in graphene were excited and probed using an infrared s-SNOM, as shown in Fig. 1(a). Infrared light at 10.6 μm or ~6 μm was focused onto the apex of a gold-coated atomic force microscope (AFM) tip with a radius of 25 nm, which enabled optical excitation of 2DSPs in graphene. The excited 2DSPs propagated in graphene and got reflected at the edge. The back-reflected 2DSPs wave interfered with the excited wave underneath the tip, which modified the intensity of the tip-scattered infrared radiation measured by an HgCdTe detector in the far field. Shown in Fig. 1(b) is a near-field optical image of 2DSPs near the edge of an hBN-sandwiched graphene sample. Due to the edge-reflection, a standing-wave-like interference pattern is clearly observed. We measured the edge reflection in a spectral range from 1570cm^{-1} to 1620cm^{-1}, and found similar interference patterns with shorter 2DSP wavelengths at higher frequencies, as shown in Fig. 1(c). In both Fig. 1(b) and (c), we can see that scattered infrared light intensity varies periodically, with intensity peaks appearing at the positions of constructive interference. The detailed interference pattern, however, cannot be described by a simple reflection with 0 or π phase shift. First, the separation between the first and second peak is significantly different from those between other adjacent peaks, which have a nearly constant value as denoted by the equally spaced dashed lines. Second, the intensity of the peaks does not have a smooth monotonic decay. Instead, it shows an interesting even-odd oscillation where the odd peaks tend to have higher intensities compared with adjacent even peaks. These behaviours are similar to those reported in previous studies of hBN-encapsulated graphene, but their origin was not well understood, and is often attributed to extrinsic

effects such as edge-induced excitation of 2DSP[7]. However, a recent work has shown that the even-odd peak oscillation is not due to the edge excitation because there is no polarization dependence[22], but the origin of the even-odd peak oscillation still remains unknown. Here we show that such behaviours are intrinsic to edge reflection of 2DSPs due to the existence of near-field evanescent waves.

We investigate the edge reflection theoretically using a combination of analytical calculations and finite-difference time-domain (FDTD) simulations. We consider a semi-infinite 2D metal plane located at y=0, as shown in Fig. 2(a). By solving Maxwell's equation numerically using the FDTD method, we investigate near-field profiles formed by the edge-reflection. Figure 2(b) shows the profile of y-component of electric field E_y. The FDTD simulation reproduces main features observed experimentally. It shows that the separation between the first and second peak is larger than the other peak separations. In addition, it shows that the near-field pattern can change significantly with the sample-tip position as shown in Fig. 2(c): a pronounced asymmetry between the even and odd peak appears with increased sample-tip separation.

To better understand these anomalous behaviours at the edge, we carried out analytical calculation by modelling the edge reflection problem as a diffraction of surface-bound EM waves that occurs at the interface of a discontinuous surface conductivity, like guided wave experiences a diffraction at an open end of the waveguide[28,29]. The edge-reflection then can be dealt with as a boundary problem of Maxwell's equations. For strongly confined 2DSP, direct scattering to the far field is negligible, and a key component in this diffraction problem is the non-propagating near-field evanescent wave. Including the evanescent wave, we can write y-component of electrical field for the region with graphene (x>0 in Fig. 2(a))

as $E_y^{total} = E_y^{inc} + E_y^{ref} + E_y^{ev}$, where the first and second terms on the right-hand-side stand for incident and reflected 2DSPs, respectively, and E_y^{ev} is the near-field evanescent wave. In the free-space region (x<0), there is only the evanescent wave E_y^{ev}. Then we apply boundary matching at x=0 and obtain every field profile including reflection coefficient. Figure 2(d) shows analytically calculated E_y field profile (See Supplementary Information for details). Our analytic calculations show excellent agreement with FDTD results displayed in Fig. 2(b).

The presence of the near-field evanescent wave significantly modifies the edge reflection of 2DSP, both in the reflection phase and the field distribution profile. First, we provide a physical picture for the reflection phase shift of 2DSPs based on the analytic result. The presence of the evanescent wave means that the electromagnetic energy will be stored in the evanescent wave first, and then get back reflected. As a result, it will experience a phase delay related to the evanescent wave, which is well known as the Goos-Hänchen phase shift in total internal reflection[18,19]. To characterize the Goos-Hänchen phase shift quantitatively, we define effective wave impedance Z_{eff} for the evanescent wave. For a plane wave, the impedance is simply the ratio of the transverse component of the electric and magnetic fields. Based on our analytical calculation, the effective impedance of evanescent wave at the edge of 2DSP can be written as

$$Z_{eff}^{-1} \approx \alpha \frac{\int_{-\infty}^{\infty} dk_y Z_{pw}^{-1} \left| A\left(k_y\right) \right|^2}{\int_{-\infty}^{\infty} dk_y \left| A\left(k_y\right) \right|^2} = \alpha \left\langle Z_{pw}^{-1} \right\rangle$$

where $A(k_y)$ and $Z_{pw} \equiv Z_0 k_x / k_0$ respectively are amplitude and impedance of a plane-wave component of Fourier-transformed 2DSPs, α is a constant, and $k_x \equiv \sqrt{k_0^2 - k_y^2}$

where k_0 is the photon momentum in the free-space (See SI for details). The reflection coefficient R can be expressed as

$$R = \frac{Z_{eff} - Z_{sp}}{Z_{eff} + Z_{sp}}$$

where $Z_{sp} \equiv Z_0 q_x / k_0$ is the wave impedance of 2DSPs, and Z_{eff} is the effective impedance of the evanescent wave. Note that the expression is exactly the same as the case where a plane wave gets reflected at a boundary.

Shown in Fig. 3(a) is the magnitude and phase of R with varying momentum ratio q_x/k_0. For strongly confined 2DSP, (i.e. $q_x/k_0 >> 1$), the magnitude saturates to 1. This means that far-field scattering is negligible, and the edge-reflection of 2DSPs is nearly total internal reflection, of which the phase change can be defined in terms of Goos-Hänchen phase shift[19],

$$\phi_{G-H} \equiv 2 \arctan\left(iZ_{sp} / Z_{eff}\right).$$

When $q_x/k_0 >> 1$, this converges to 0.25π (see SI for details). Now we compare our theoretical prediction to our experimental measurements of gated graphene on SiO_2/Si substrate. Although graphene on SiO_2/Si substrates has a lower plasmon quality factor than that of hBN encapsulated graphene, it allows us to determine the graphene edge reliably through topography measurements and obtain quantitative information on the reflection phase shift. Figure 3(b) shows a representative near-field infrared microscopy image measured with a gate voltage of -100 V at an excitation photon wavelength at 10.6 μm. From the plasmon line-profiles shown in Fig. 3(c), we can determine the plasmon wavelength reliably from oscillation peak positons. The reflection phase can then be obtained by examining the distance between the third reflection peak and the graphene

edge (see Supporting Information). We measured the plasmon reflection phases as a function of the gate voltage from -100 to -50 V, as shown in Fig. 3(d) and 3(e). Within this range, graphene remains highly doped and the plasmon features are strong and suitable for the phase determination. Fig. 3(d) shows that q_x/k_0 ratio is much larger than 1, which should have a constant 0.25π reflection phase based on our analytic theory. Shown in Fig. 3(e) are the experimentally extracted phase shifts which are in good agreement with our theoretical prediction.

Next we examine the effect of evanescent wave on the near-field profile and explain the even-odd peak oscillations. Fig. 4(a) shows separated electric field profiles of the evanescent waves $|E_y^{ev}|$ and the propagating 2DSPs waves $|E_y^{sp}|$, of which the total electrical field $|E_y^{total}|$ consists. The total field is strongly distorted by the evanescent waves, and, as we have seen in Fig. 1(d), there is oscillation in peak heights. The origin of this even-odd peak oscillation can be found from the phase of the evanescent waves shown in Fig. 4(b). The evanescent wave basically has a constant phase along the *x*-direction, whereas the standing wave formed by incident and back-reflected 2DSPs has periodic phase alternations. The interference between the evanescent wave and the standing wave of 2DSPs therefore yields constructive (destructive) interference with odd- (even-) numbered peaks. This behaviour is clearly presented in Fig. 4(c). In addition, the even-odd peak oscillation exhibits strong height dependence, and it becomes more prominent with increased tip-sample distance, as shown in Fig. 4(c). The 2nd peak can even disappear at a specific height where pure 2DSPs has decayed sufficiently. This behaviour is in good agreement with our experimental results on hBN-encapsulated graphene sample (Fig. 4d). In our experiment, the smallest tip-graphene separation is 12nm due to the existence of the

top hBN layer. This relatively large tip-graphene separation makes the intensity oscillation between even and odd peaks particularly strong. Because the near-field distribution profile scales with the wavelength of 2DSP, the effective tip-graphene separation (scaled by the 2DSP wavelength) can be varied by changing 2DSP wavelength for a constant hBN thickness. This is realized in our experiment by tuning the excitation photon frequencies around the hBN phonon resonance. Figure 4(d) displays the near-field profiles of the 2DSP edge-reflection for different excitation frequencies. It was apparent that the strongest even-odd peak oscillation occurs for the shortest surface polariton wavelength (excitation at 1660 cm^{-1}), where the even oscillation peaks are barely distinguishable. This asymmetry between even and odd peaks becomes weaker for longer 2DSP wavelengths, such as for excitation at 1580 cm^{-1}. The good agreement between theory and experiment in the fine structure of near-field profile further confirms the validity of our analytic theory for edge-reflection of 2DSPs.

In summary, we have investigated both experimentally and theoretically the edge-reflection of 2DSPs in graphene. Experimentally, we have measured a specific phase shift of reflected graphene plasmon and even-odd peak oscillations in the near-field profile. Theoretically, we have developed an analytic theory to describe the reflection of 2DSP at an abrupt edge, which reveals the importance of near-field evanescent wave close to the edge. This evanescent wave leads to a Goos-Hänchen phase shift of 0.25π in 2DSP reflection and the asymmetry between the even and odd peaks in electric field profile. Our results are not limited to 2D plasmons, but are important for understanding edge reflection of all 2D polaritons, including phonon polaritons in ultrathin boron nitride flakes and exciton polariton in two-dimensional semiconductors.

Methods summary

Sample preparation

For the graphene/SiO_2/Si sample, monolayer graphene was first exfoliated on SiO_2/Si substrates and then gold electrodes were deposited. To prepare the hBN/graphene/hBN sandwich structure, the exfoliated graphene was transferred hBN flake using direct pick-up method (ref), yielding the graphene/hBN heterostructure. Another boron nitride flake was also transferred onto to the graphene/hBN samples to form hBN/graphene/hBN sandwich structure. Gold electrodes were deposited afterwards to tune them to high doping level to achieve strong plasmon response.

Near-field optical measurement

Near-field optical measurement was carried out at Beamline 5.4 in the Advanced Light Source (ALS) of Lawrence Berkeley National Laboratory and on homebult s-SNOM. A quantum cascade laser beam with central wavelength ~6.13 μm or a CO_2 laser with wavelength 10.6 μm was focused onto an Au coated tip of a commercial AFM (Innova, Bruker). The backscattered light from the AFM tip is collected at the far-field and focused onto an MCT detector (KLD-0.1-J1, Kolmar). The AFM is operated in tapping mode with an amplitude ~80 nm, and the tip-scattered signal is demodulated at thrice the tip-oscillation frequency (typically 250–300 kHz) with a lock-in amplifier (HF2Li-MF, Zurich Instruments).

FDTD numerical calculations

We used home-made FDTD program to perform numerical calculations. For the excitation

of 2DSPs, we considered $\lambda_0/20{,}000$ thick metal slab possessing a pure-real permittivity $\varepsilon = -127.3+0i$ to simplify the problem by considering lossless propagation of 2DSPs. In this configuration, the propagating momentum of 2DSPs is approximately calculated as $k_{x,sp} \approx 2/h|\varepsilon| \approx 50k_0$ where h is the thickness of the slab[30].

References

1. Ju, L. *et al.* Graphene plasmonics for tunable terahertz metamaterials. *Nat. Nanotechnol.* **6,** 630–4 (2011).
2. Yan, H. *et al.* Infrared spectroscopy of tunable Dirac terahertz magneto-plasmons in graphene. *Nano Lett.* **12,** 3766–3771 (2012).
3. Yan, H. *et al.* Tunable infrared plasmonic devices using graphene/insulator stacks. *Nat. Nanotechnol.* **7,** 330–334 (2012).
4. Fei, Z. *et al.* Gate-tuning of graphene plasmons revealed by infrared nano-imaging. *Nature* **487,** 82–85 (2012).
5. Chen, J. *et al.* Optical nano-imaging of gate-tunable graphene plasmons. *Nature* 3–7 (2012).
6. Zhou, W. *et al.* Atomically localized plasmon enhancement in monolayer graphene. *Nat. Nanotechnol.* **7,** 161–165 (2012).
7. Woessner, A. *et al.* Highly confined low-loss plasmons in graphene–boron nitride heterostructures. *Nat. Mater.* **14,** 421–425 (2014).
8. Principi, A. *et al.* Plasmon losses due to electron-phonon scattering: The case of graphene encapsulated in hexagonal boron nitride. *Phys. Rev. B* **90,** 1–14 (2014).
9. Con, H. *et al.* Highly Confined Tunable Mid-Infrared Plasmonics in Graphene

Nanoresonators. *Nano Lett.* **13,** 2541–2547 (2013).

10. Bonaccorso, F., Sun, Z., Hasan, T. & Ferrari, A. C. Graphene Photonics and Optoelectronics. *Nat. Photonics* **4,** 611–622 (2010).
11. Dai, S. *et al.* Tunable Phonon Polaritons in Atomically Thin van der Waals Crystals of Boron Nitride. *Science (80-.).* **343,** 1125–1129 (2014).
12. Shi, Z. *et al.* Amplitude- and Phase-Resolved Nanospectral Imaging of Phonon Polaritons in Hexagonal Boron Nitride. *ACS Photonics* **2,** 790–796 (2015).
13. Kim, J. *et al.* Ultrafast Generation of Pseudo-magnetic Field for Valley Excitons in WSe2 Monolayers. *Science (80-.).* **346,** 1205–1208 (2014).
14. Li, D. *et al.* Electric-field-induced strong enhancement of electroluminescence in multilayer molybdenum disulfide. *Nat. Commun.* **6,** 7509 (2015).
15. Mak, K. F., He, K., Shan, J. & Heinz, T. F. Control of valley polarization in monolayer MoS2 by optical helicity. *Nat. Nanotechnol.* **7,** 494–498 (2012).
16. Chakraborty, C., Kinnischtzke, L., Goodfellow, K. M., Beams, R. & Vamivakas, a. N. Voltage-controlled quantum light from an atomically thin semiconductor. *Nat. Nanotechnol.* **10,** 507–511 (2015).
17. Ye, Z. *et al.* Probing Excitonic Dark States in Single-layer Tungsten Disulfide. *Nature* **513,** 214–218 (2014).
18. Jackson, J. D. *Classical Electrodynamics 3rd Edition*. (John Wiley & Sons, INC., 1999).
19. Chuang, S. L. *Physics of Optoelectronic Devices*. (John Wiley & Sons, INC., 1995).
20. Zia, R., Chandran, A. & Brongersma, M. L. Dielectric waveguide model for guided surface polaritons. *Opt. Lett.* **30,** 1473–1475 (2005).

21. Gerber, J. A., Berweger, S., O'Callahan, B. T. & Raschke, M. B. Phase-resolved surface plasmon interferometry of graphene. *Phys. Rev. Lett.* **113,** 1–5 (2014).

22. Ni, G. X. *et al.* Ultrafast optical switching of infrared plasmon polaritons in high-mobility graphene. *Nat. Photonics* **10,** 244–248 (2016).

23. Nikitin, A. Y., Low, T. & Martin-Moreno, L. Anomalous reflection phase of graphene plasmons and its influence on resonators. *Phys. Rev. B* **90,** 1–5 (2014).

24. Thongrattanasiri, S., Koppens, F. H. L. & Garcıa De Abajo, F. J. Complete optical absorption in periodically patterned graphene. *Phys. Rev. Lett.* **108,** 1–5 (2012).

25. Gao, W. *et al.* Excitation and active control of propagating surface plasmon polaritons in graphene. *Nano Lett.* **13,** 3698–3702 (2013).

26. Jablan, M., Buljan, H. & Soljačić, M. Plasmonics in graphene at infrared frequencies. *Phys. Rev. B* **80,** 1–7 (2009).

27. Llatser, I. *et al.* Graphene-based nano-patch antenna for terahertz radiation. *Photonics Nanostructures - Fundam. Appl.* **10,** 353–358 (2012).

28. Chandran, A., Barnard, E. S., White, J. S. & Brongersma, M. L. Metal-dielectric-metal surface plasmon-polariton resonators. *Phys. Rev. B* **85,** 1–9 (2012).

29. Gordon, R. Light in a subwavelength slit in a metal: Propagation and reflection. *Phys. Rev. B* **73,** 8–10 (2006).

30. Alù, Andrea, Engheta, N. Optical Nanotransmission Lines : Synthesis of Planar Left-Handed Metamaterials in the Infrared and Visible Regimes. *J. Opt. Soc. Am. B* **23,** 571–583 (2006).

Acknowledgements

This work was mainly supported by Office of Basic Energy Science, Department of Energy under contract No. DE-AC02-05CH11231 (Sub-wavelength Metamaterial program). J.K. was supported in part by Basic Science Research Program through the National Research Foundation of Korea (NRF) funded by the Ministry of Education (NRF-2013R1A1A2011757).

Author contributions

J.K., Z.S., and F.W. conceived the project. J.K. developed the theory and performed the numerical calculations. S.W., Z.S., and W.Z. performed the near-field IR measurements. J.K., S.W., and Z.S. prepared the figures. All authors analysed the data and contributed to writing the manuscript.

Competing financial interests

There is no competing financial interests.

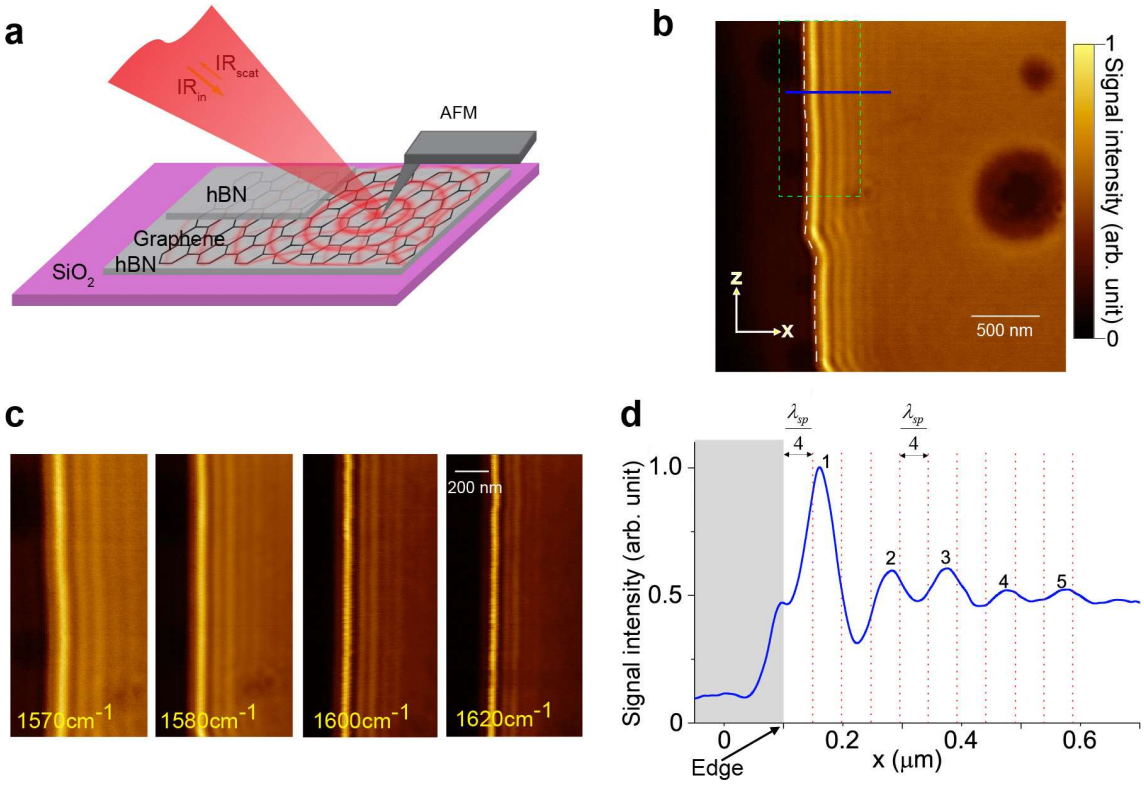

Figure 1. Near-field measurement of 2DSPs in graphene sandwiched in hBN flakes. a, Infrared light is incident onto a sharp AFM tip that allows excitation of surface plasmon in graphene. When 2DSPs meet the crystal edge, there occurs the edge-reflection. **b**, Experimentally measured near-field map of interference pattern between incident and edge-reflected 2DSPs. White dashed line indicates the edge of the graphene, identified by the topography (see SI for details). **c**, Frequency-dependent standing wave pattern formed by the edge-reflection. The maps are taken in the area of green dashed-rectangle in **b**. **d**, Cross-cut profile of interference pattern taken along the blue line in **b**. Red dotted-lines denote positions of which the distance from the edge is multiple integer of quarter SP wavelength. The grey area is outside the graphene region.

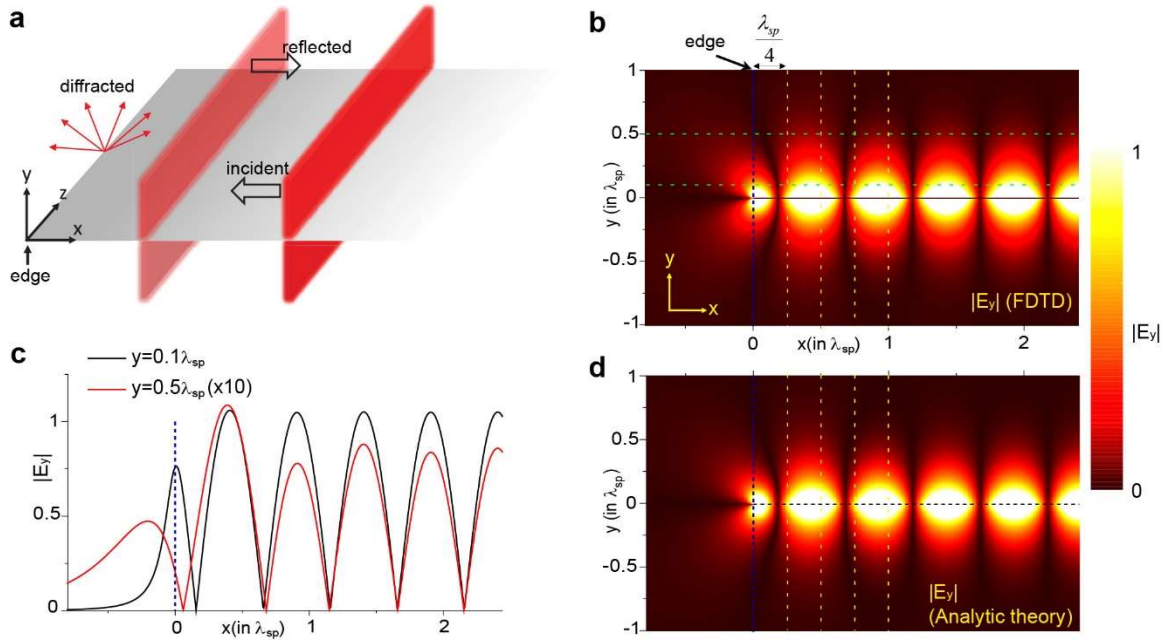

Figure 2. Analytical and numerical results of edge-reflections. a, Schematics of the edge-reflection. Anti-symmetric 2DSPs on the freestanding thin metal is incident along the *x*-axis. We assumed that the edge-reflection results in not only reflected 2DSPs but also additional evanescent field near the edge. **b**, FDTD-calculated edge-reflection. Profile of amplitude of *y*-component electric field $|E_y|$ is given. **c**, Crosscut field profiles of $|E_y|$ at two different height indicated by green horizontal dotted lines in **b**. **d**, Edge-reflection from analytic calculations. Blue dotted lines in **b, c,** and **d** denote the edge of the metal film. Yellow doted lines in **b** and **d** indicate where the distance from the edge is integer multiple of quarter 2DSPs wavelength.

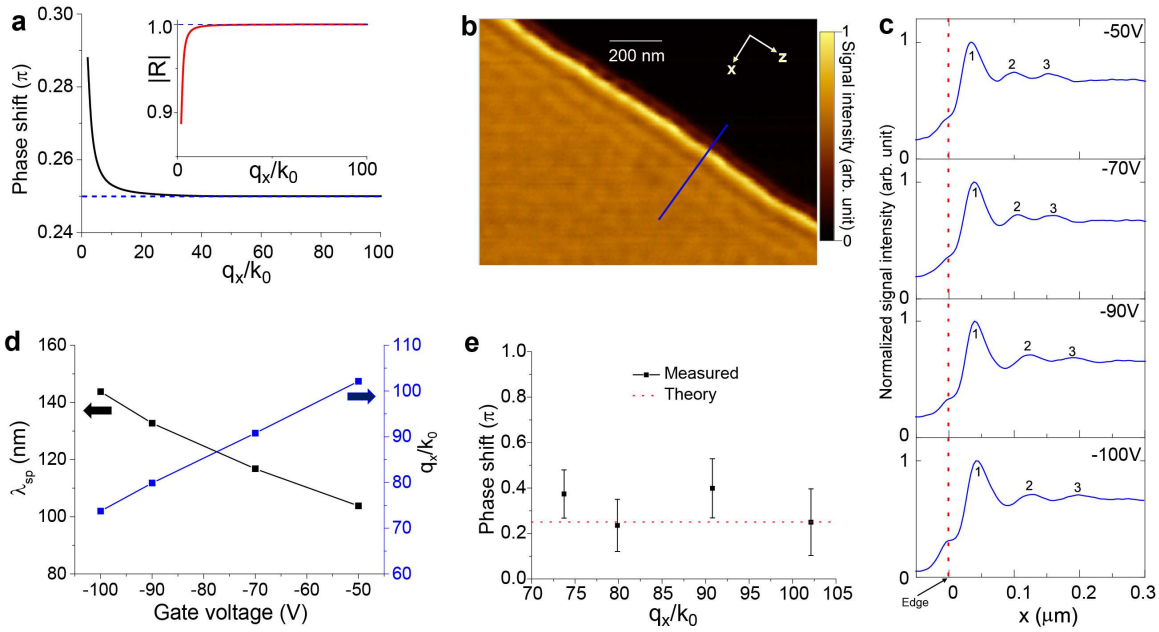

Figure 3. Phase shift of edge-reflected 2DSPs. a, Analytically-calculated phase shift. Blue dotted-line is the value of 0.25π. Amplitude of reflection coefficient R is given in the inset. As $q_x >> k_0$, the edge-reflection behaves like a total internal reflection with a constant phase shift. **b**, Measured 2DSP map of gated graphene on SiO_2/Si substrate, with gating voltage of -100 V at excitation wavelength 10.6 μm. **c**, Gate-dependent crosscut profiles of 2DSPs, and **d**, corresponding polariton wavelengths and momenta. **e**, Phase shift extracted from **c** (See Supporting Information for details).

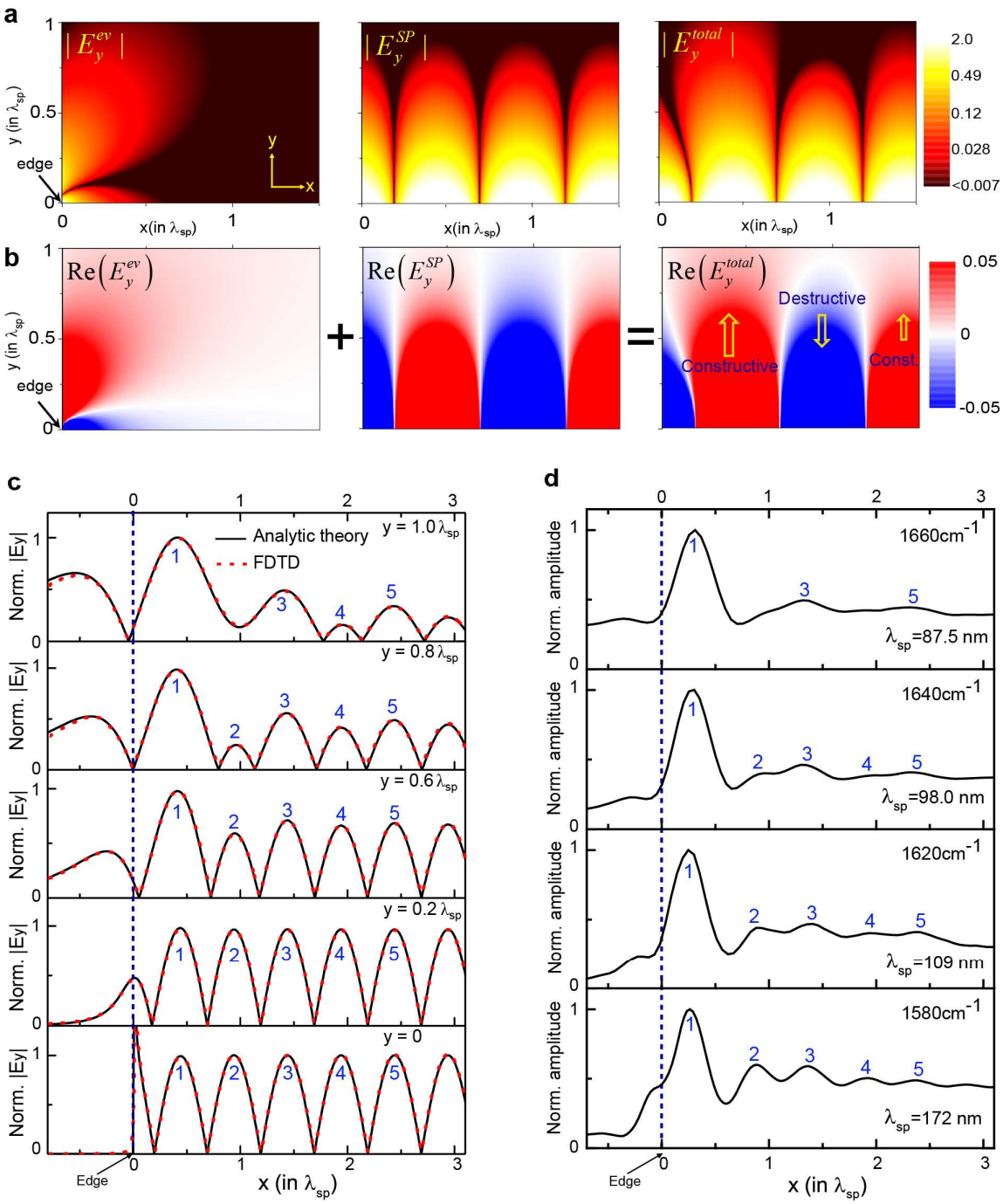

Figure 4. Even-odd peak oscillations. a, Separated description of evanescent fields and pure 2DSPs near the edge. Due to their interferences, the near-field profile of the total field is shown to be distorted. **b**, The origin of even-odd oscillations. When *y* is not so close to the surface, the evanescent field has nearly constant phase along *x*-direction whereas that

of 2DSPs alternates. Constructive (destructive) interferences therefore occur only at even- (odd-) numbered antinodes, respectively. **c**, Analytically and numerically calculated field profiles at selected heights. As height increases, the even-odd peak oscillation gets more conspicuous. **d**, Experimental results from hBN/graphene/hBN encapsulated sample with four different excitation frequencies. Since the 2DSPs have shorter wavelengths at higher frequencies, the λ_{sp}-normalized distance between the tip and the sample surface in a higher frequency is larger than that in a lower frequency. All plots in **c** and **d** are normalized by their first peak amplitude, respectively.